Chapter 5

# Long-Period Fiber Gratings in Active Fibers

David Krčmařík, Mykola Kulishov and Radan Slavík

Additional information is available at the end of the chapter

http://dx.doi.org/10.5772/53008

## 1. Introduction

Traditionally, long period fiber gratings (LPG) are made in passive optical fibers that have negligible loss. However, loss or gain that can be controlled via optical pumping adds a new degree of freedom and – as will be shown in this chapter – brings many new and interesting properties.

From the historical perspective, the first attempt to combine the fiber gain and LPG filtering characteristics was for gain flattening of an Erbium-doped fiber (EDF) amplifier by inscribing LPG directly into the active fiber [1]. At the same time, theoretical studies [2,3] showed that a proper level of loss/gain in the fiber core or cladding can modify the LPG transmission characteristics. Significant theoretical and experimental body of work has been published since with new emerging applications appearing.

In this chapter, we investigate the new phenomena brought by the presence of the loss/gain [2,3]. Following this, we look on practical possibilities how to obtain required gain in active optical fibers and show how to analyze such structures, in which (incoherent) noise from an amplifying fiber is simultaneously generated and diffracted at the LPG [4]. Finally, we discuss possible application of the LPG in active fibers.

## 2. Theoretical analysis

First, we analyze LPG using standard coupled mode theory in which we consider that the refractive index is a complex number in which the imaginary part represents the gain/loss. Following this analysis, we show approaches into rigorous modeling of the active gain medium that contains an LPG, including the spontaneous emission and amplified spontaneous emission generation, propagation, and diffraction.

## 2.1. Coupled mode equations considering gain/loss

Similarly to an LPG in a gain/loss-less fiber, LPG assists coupling between the core and a cladding mode at the wavelength for which the phase matching condition is satisfied for real part of the mode propagation constants:

$$\mathrm{Re}\left(\beta^{cl}\right) = \mathrm{Re}(\beta^{co}) - \frac{2\pi}{\Lambda}, \tag{1}$$

where $\beta^{cl} = (2\pi/\lambda)n^{cl}_{eff} + j\alpha^{cl}$ and $\beta^{co} = (2\pi/\lambda)n^{co}_{eff} + j\alpha^{co}$ are the propagation constants of the interacting cladding and core modes, respectively, $\lambda$ is the wavelength, $\Lambda$ is the grating period, $n^{cl}_{eff}$ and $n^{co}_{eff}$ are the effective refractive indices of the interacting cladding mode and the core mode, $\alpha^{cl}$ and $\alpha^{co}$ are the absorption (when positive) or amplification (when negative) factors of the cladding and the core modes, respectively. Propagation constants for the core and cladding modes can be straightforwardly calculated, especially when considering a step-index fiber refractive index profile [4-6]. The strength of the coupling between the two modes depends on the coupling coefficient calculated as a confinement factor between the field of the two interacting modes [7]:

$$\kappa(z) = 0.5\omega\varepsilon_0 n^2 \sigma(z) \int_0^{2\pi} d\phi \int_0^{r_1} [r(E_r^{cl} E_r^{co*} + E_\varphi^{cl} E_\varphi^{co*})]dr \tag{2}$$

where $\omega$ is the angular frequency, $\varepsilon_0$ is the permittivity of vacuum, $\sigma(z)$ is the LPG index modulation amplitude, $E_r$ and $E_\phi$ are the radial and azimuthal parts of electric field. The asterisk signifies complex conjugate value. For non-uniform LPGs the index modulation amplitide generally varies along the fiber, so it depends on the distance z from the LPG input. In the following text we consider only LPGs which are uniform ($\sigma(z)=const$ over the entire LPG length).

The mode coupling process along the LPG is described by the following coupled mode equations [7]:

$$\frac{dA}{dz} = i\kappa B \exp(-2i\delta z), \tag{3}$$

$$\frac{dB}{dz} = i\kappa A \exp(2i\delta z), \tag{4}$$

$$\delta = \frac{\beta^{co} - \beta^{cl}}{2} - \frac{2\pi}{\Lambda}, \tag{5}$$

where $A(z)$ and $B(z)$ are slowly varying envelopes of the core mode and the interacting cladding mode, and $z$ is the coordinate originated at the LPG input. The solution of these equations for a uniform LPG of length $L$ and for the initial condition of input signal launched in the core mode only ($A(0) = 1$ and $B(z) = 0$) can be written in the form of the amplitude core-to-core mode transmission [2]:

$$t = \frac{A(L)}{A(0)} = \left[ \cos(\gamma L) + j\frac{\delta}{\gamma}\sin(\gamma L) \right] \exp\left[ jL\left(\beta^{co} - \delta\right) \right], \tag{6}$$

where $\gamma$ is:

$$\gamma = \sqrt{\delta^2 + \left|\kappa\right|^2}. \tag{7}$$

## 2.2. Condition for critical coupling

In a standard fiber like SMF-28, propagation losses are low and can be completely neglected over few centimeters, which is a typical LPG length, even for high order cladding modes (provided the protective high-refractive index fiber jacket is stripped off). Therefore, the long period index perturbation along the fiber length provides constant optical power exchange between the coupled modes. An optical signal launched into the core at the LPG resonance wavelength will be completely coupled by the LPG into the cladding mode and then it will be completely coupled back into the core. This process will be repeated again and again as long as long-period perturbation is induced along the fiber. At the LPG resonance wavelength where the mismatch factor $\delta = 0$, the core-to-core mode transmission is

$$t = \cos(\kappa L). \tag{8}$$

The only way to provide full signal out-coupling from the core into the cladding mode is to terminate the LPG at discrete length values of $L = m\pi/(2\kappa)$, for $m$ = 1, 2, 3, …

As we will describe now, the performance changes completely when there is an appropriate level of loss or gain in the fiber core or cladding. For example, for the case of cladding mode loss, optical signal is getting lost there and less optical power returns back into the core. However, the situation is more complicated/interesting as shown below.

At the wavelength where the mode matching condition (Eq.(1)) is satisfied, the mismatch factor becomes purely imaginary: $\delta = -j(\alpha_{cl} - \alpha_{co})/2$. Substituting this expression for mismatch factor at the resonance wavelength into Eq.(6), and equating it to zero, we get a relationship between the grating strength, $\kappa L$, and the dimensionless loss factor, $q = (\alpha_{cl} - \alpha_{co})/(2\kappa)$:

$$t = \cos(\sqrt{1-q^2}\kappa L) + \frac{q}{\sqrt{1-q^2}}\sin(\sqrt{1-q^2}\kappa L) = 0 \tag{9}$$

The solution of Eq.(9) is presented (in dimensionless variables: $\kappa L$ and $q$) in Fig. 1. For each value of $\kappa L$ the curve gives us the optimum ratio between the attenuation and the coupling coefficient (characterized by $q$) that provides full signal light attenuation in the core mode. Thus, solution exists for any $\kappa L$, unlike for a loss-less LPG, where full coupling is possible only at discrete values of $\kappa L$. In other words, zero core mode transmission for an LPG of any strength $\kappa L$ can be found, depending on the loss/gain relations of the core and the interacting cladding modes.

It is worth analyzing which parts of the curve shown in Fig. 1 are practically attainable. For example, in a usual situation in which the core mode loss is smaller than the cladding mode loss, we get always $q>0$ and thus full coupling is possible (from Fig. 1) only for $\kappa L>\pi/2$. However, $q<0$ (and thus also full coupling at $\kappa L<\pi/2$, Fig. 1) can be, e.g., achieved by introducing loss into the core mode (that is larger than the cladding mode loss). Another interesting possibilities are considering core mode gain (q>0 and thus solutions limited to $\kappa L>\pi/2$) or cladding mode gain with the core mode unamplified (q<0 with solutions for $\kappa L<\pi/2$) [3]. The latter could be practically achieved when considering double-clad fibers used for high-power fiber lasers, in which the cladding is doped by active ions [8].

Another interesting feature when considering gain/loss of core/cladding modes is that it may reduce interference sidelobes occurring outside of the resonance, obtaining a smooth, side-lobe free transmission spectrum [2].

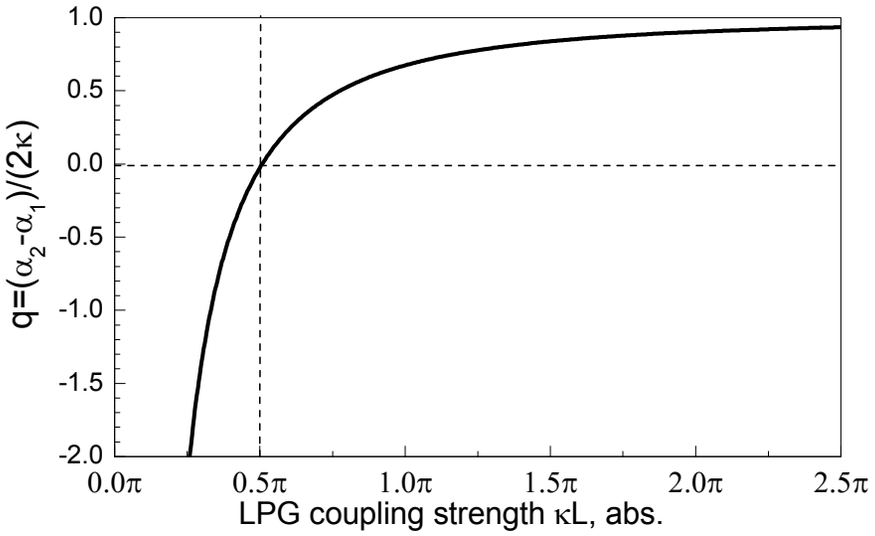


**Figure 1.** Required value of $q=(\alpha_{cl}-\alpha_{co})/(2\kappa)$ for obtaining full attenuation in the transmission spectrum of the core mode at the resonance wavelength (critical coupling) for a given LPG strength of $\kappa L$.

To provide some physical insight into the mode coupling process in the presence of gain or loss, we show the grating transmission as a function of $\kappa L$ for various values of $q=\alpha_2/2\kappa$ (for clarity, only loss/gain in the cladding mode is considered here) – Fig. 2 [3]. The conventional sinusoidal transmission of loss/gain-free grating is shown as a solid curve. We can clearly see distinct types of transmission grating behavior depending on the magnitude of loss/gain.

## 2.3. Active fibers

The analysis of LPG in active fibers is based on a combination of two processes: coupled mode interaction (characterized by Eqs.(3-4)) and mode amplification (characterized by rate equations) [4]. To observe effects described in the previous section, high concentration of Er ions is required to achieve a significant gain over a length of an LPG that is usually relatively short (cm to tens of cm). Such high Er concentrations generally lead to cluster formations and up-conversion in the EDF, which has also to be taken into account.

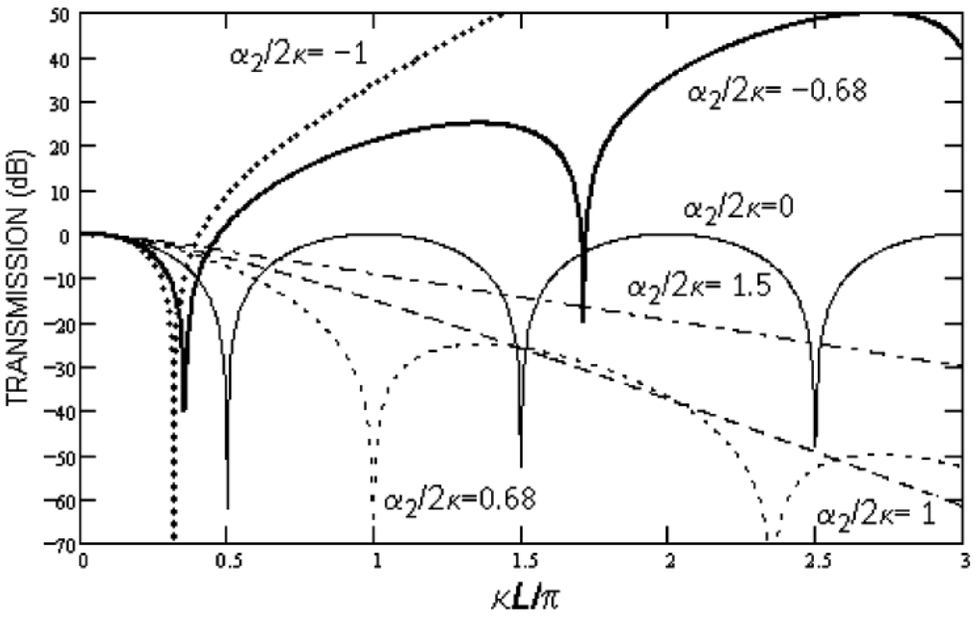


**Figure 2.** Variation of the grating transmission at the resonance wavelength with the grating strength κL for different q=$\alpha_2/2\kappa$ values.

There are several new phenomena occurring when considering not only the gain factor as in the previous part. The presence of gain/loss in the fiber with an LPG also changes resonance wavelength through modification of the effective refractive index of the coupled modes through Kramers-Kroning effect. Further, the presence of (amplified) spontaneous emission, (A)SE limits the maximum attainable transmission dip [4].

Here, the fibre is simulated by a two level system with the ground level and the meta-stable (excited) level. Due to high concentration of *Er* ions in the fibre it is necessary to take into account possible cluster formation and elevated occurrence of the up-conversion (process when the *Er* ions reach higher levels of excitation). Both cluster formation and up-conversion severely limits the maximum attainable gain for fibres with high concentration of Er ions and thus has to be considered.

In the up-conversion model we assume that the probability of the interaction of an ion with its neighbour is proportional to $N_2^2$, where $N_2$ is the number of Er ions in the excited state. Next model assumes cluster formation. In a cluster, only a single Er ion can contribute to the gain. In our analysis, clusters with more than two Er ions are not considered, as their contribution is generally negligible. In a combined model [9] the total number of ions contributing to the gain is:

$$N_2 = N_2^{SC} + N_2^P, \tag{10}$$

where $N_2^{SC}$ is an average number of single excited ions and $N_2^P$ is an average number of excited clusters. The average number of Er ions in not-excited state is $N_1 = N_{Er}-N_2$ (with $N_{Er}$ total number of Er ions). Average number of single excited ions and excited clusters is:

$$N_2^{SC} = \frac{(1-2R)N_{Er}\sum_k \frac{P_k(z)\sigma_k^a \tau_{21}\Gamma_k}{h\nu_k A_{eff}}}{1 + C_{up}(1-2R)N_2^{SC}\tau_{21} + \sum_k \frac{P_k(z)}{P_k^{IS}}}, \tag{11}$$

$$N_2^{P} = \frac{2RN_{Er}\sum_k \frac{P_k(z)\sigma_k^a \tau_{21}\Gamma_k}{h\nu_k A_{eff}}}{1 + \sum_k \frac{P_k(z)}{P_k^{IS}} + \sum_k \frac{P_k(z)\sigma_k^a \tau_{21}\Gamma_k}{h\nu_k A_{eff}}}, \tag{12}$$

where

$$P_k^{IS} = \frac{h\nu_k A_{eff}}{(\sigma_k^a + \sigma_k^e)\tau_{21}\Gamma_k}. \tag{13}$$

In the above equations $R$ is a percentage of ions in clusters, $P_k$ is the peak power of signals and pump on $\nu_k$ frequencies, $\tau_{21}$ is the metastable state lifetime, $h$ is the Planck constant, $A_{eff}$ is the effective core area and $\sigma_k^a$ with $\sigma_k^e$ are the absorption and emission cross-sections defined in the characteristics of the fiber. $C_{up}$ [10] is the concentration independent and host dependent constant in $m^3/s$. Constant $C_{up}$ can be determined by fitting the measured data. $\Gamma_k$ is the overlap integral between the doped area and the optical mode field [11].

In an active medium we can observe a refractive index change due to the pump power. This translates into the slight wavelength shift of the coupling wavelength. The refractive index change is given by [12]:

$$\delta n = \left( \frac{\sigma_e' N_{Er}\alpha}{1+\alpha} - \frac{\sigma_a' N_{Er}}{1+\alpha} \right) \frac{\lambda\Gamma(\lambda)}{4\pi}, \tag{14}$$

$$\alpha = \frac{\sum_k P_k(z)}{P_{thr}}, \tag{15}$$

where $P_{thr}$ is the threshold power for which the number of Er ions in the ground state is the same as in the meta-stable state ($N_1$=$N_2$). $P_k$ sums both the signal powers and the pump powers in forward and backward directions. Since the pump propagates mainly in the core, we have neglected any refractive index changes in the cladding. Real parts of the absorption coefficient $\sigma_a'$ and the emission coefficient $\sigma_e'$ are computed from $\sigma_a$ and $\sigma_e$ through Kramers-Kroning relations.

To include the active medium into the coupled-mode theory, it is necessary to define the signal absorption coefficient $g_a(z, \nu)$, signal emission coefficient $g_e(z, \nu)$ and pump absorption coefficient $\alpha_p$ [13]:

$$g_a(z,\nu) = \sigma^a(\nu)N_1(z)\Gamma(\nu) - BL, \tag{16}$$

$$g_e(z,\nu) = \sigma^e(\nu)N_2(z)\Gamma(\nu), \tag{17}$$

$$\alpha_p(z,\nu_p) = \sigma_p^a(\nu_p)N_1(z)\Gamma_p(\nu_p) + BL, \tag{18}$$

where the index $p$ is attributed to the variables corresponding to the pump, and $BL$ is the background loss. Here we assume a fiber with Er ions doped in the core only and thus that only the core mode is amplified since most of the power of the cladding modes propagates in the cladding. The core mode is amplified according to:

$$\frac{dP_A}{dz} = (g_e - g_a)P_A, \tag{19}$$

where $P_A$ is the core mode intensity. The pump is then described similarly by:

$$\frac{dP_p^{\pm}}{dz} = -\alpha_p P_p^{\pm}. \tag{20}$$

The signs ± mean forward and backward pumping.

## 2.4. Amplified spontaneous emission and modes of pumping

As described above, more careful approach has to be taken for ASE. The coupled mode equations, Eqs.(3-4), are amplitude and phase dependent (describing coherent interaction), while the rate equations represented by Eqs.(16-20) are power intensity-dependent only (describing an incoherent interaction).

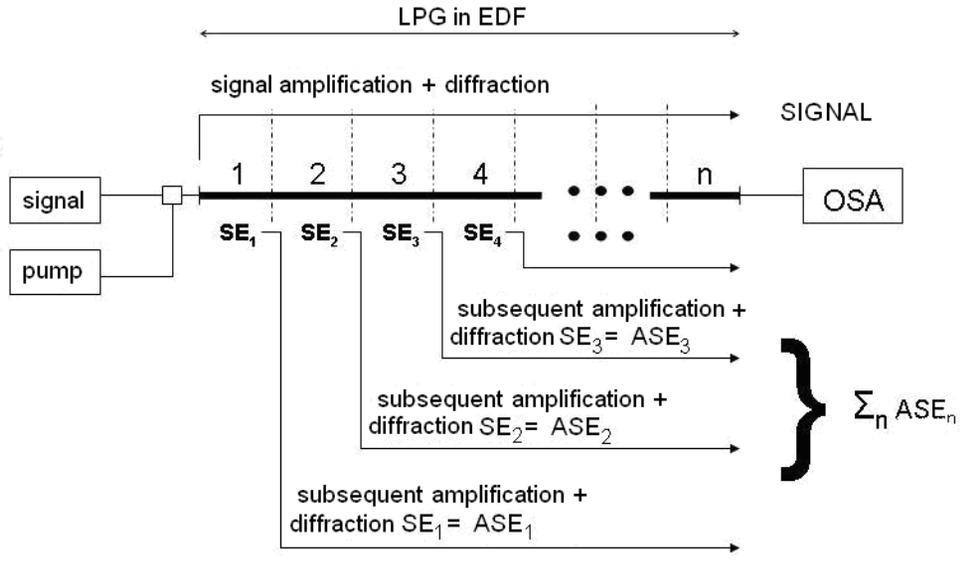


**Figure 3.** Description of SE and ASE treatment (SE – spontaneous emission, ASE – amplified spontaneous emission, OSA – optical spectrum analyzer).

ASE is seeded along the entire EDF length by spontaneous emission (SE) and subsequently amplified. In a standard EDF analysis, the fiber is divided into $n$ segments first, the considered spectral bandwidth is divided into slots and each spectral component is propagated separately. Subsequently, the noise present at the input of the $i$-th segment, $i$=1, 2,..$n$ (SE generated in the ($i$-1)-th segment and ASE amplified in the ($i$-1)-th segment) is amplified (forming ASE at the output of the $i$-th segment) and summed with SE generated in the $i$-th segment. Thus, at the output, the ASE is represented by a single number (for each spectral component). Here, we divide the fiber in the same manner as described above. However, we have to prevent summing of SE that was generated at different positions along the LPG: the SE generated at the beginning of the fiber undergoes diffraction along the entire length of the LPG, SE generated in its middle is diffracted at one half of the LPG, while the SE generated at its end is not diffracted at all. Thus, we take SE generated in the first segment and subsequently amplify it and diffract along the full length of the LPG. We continue similarly with the SE generated in the 2nd, 3rd … nth segments. As a result, we have $n$ contributions of the SE+ASE at the output (each coming from SE generated in the $i$-th segment, $i$=1,2..$n$ and subsequently amplified in the $n$-$i$ segments) at the output. These contributions are incoherent (as each of them contains photons generated by SE) and thus can be summed in power intensity at the output, representing the ASE total power (for each spectral component). This approach is graphically shown in Fig. 3.

In practice, we generate SE and propagate ASE within each segment according to the equation:

$$\frac{dP_{ASE}^{\pm}}{dz} = \pm 2h\nu(\Delta\nu)g_e \pm (g_e - g_a)P_{ASE}^{\pm}, \tag{21}$$

where $\Delta\nu$ is the frequency slot. At the end of the segment the resulting ASE gets diffracted and new SE starts to arise at the beginning of the next segment.

Finally, we implemented also analysis for the contra-directional pumping configuration. In this scheme, the pump and the signal are propagated in opposite directions. For this configuration, the simulated data were obtained iteratively [4].

An example of the results using the theoretical analysis (populations of the meta-stable levels $N_2$ and ground levels $N_1$ of the EDF together with the pump power) is shown in Fig. 4. Here, we used parameters of the EDF later used in experiments – it is Liekki Er80-8/125 – more details can be found in Section 3.

Detailed analysis presented in [4] Fig. 5) reveals that optimal pumping scheme has to be chosen according to a specific application. Backward pumping is better when we want to limit the nonlinearities caused by an excessive power at the beginning of the fiber. On the other hand forward pumping shows better results for ASE suppression. For parameters considered, the LPG was always pumped relatively uniformly along its length. Therefore the transmission at the resonance wavelength is expected to be limited by the ASE formation rather than the non-uniform LPG strength that would be due to non-uniform pumping along the grating.

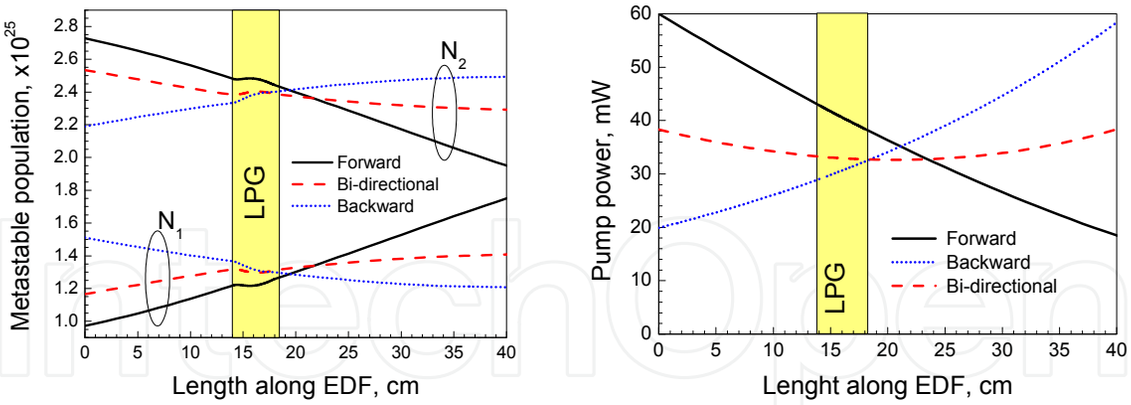


**Figure 4.** $N_1$ and $N_2$ populations (left) and pump power (right) along 40-cm long EDF sample with a 5-cm long LPG inscribed [position shown in the graphs] for total pump power of 60 mW and the input signal power of 100 μW.

## 3. Choice of EDF and fabrication techniques

Most of commercially-available EDFs have relatively high numerical aperture (0.2-0.4), which helps in obtaining good performance of these fibers. This, however, requires LPGs with sub-100-μm period, as the effective refractive index of the core mode is significantly higher than in low-numerical aperture fibers (e.g., telecom SMF-28 with numerical aperture of 0.12). Unfortunately, this is prohibitive for $CO_2$ [14] and arc [15] LPG inscription techniques – both of them operate on a principle of a local heating of the fiber and it is difficult to heat a fiber with 125 μm diameter over length significantly shorter than that. The techniques suitable are UV-writing [16] and fs-laser writing [17]. However high-gain EDF are doped with Al or P rather than Ge that is normally responsible for high UV photosensitivity. Thus, fs writing [17] seems as the most suitable method. However, to the best of our knowledge, this technique has not been used yet to fabricate LPG in EDFs; e.g., in [17], fs-writing was used for fiber Bragg grating fabrication.

In order to observe effects described in our theoretical analysis, e.g., tuning of the mode coupling interaction strength, it is necessary to provide enough gain across the LPG length that is typically 3-20 cm long. Practically, values of at least several dB per the LPG length are required, which is somehow more than in most commercially-available EDFs.

Fortunately, there are commercially available fibers that have low numerical aperture allowing use of relatively low cost techniques such as $CO_2$ and arc that do not require UV-photosensitivity and have high gain per unit length (tens of dB per meter). An example is Er80-8/125 from Liekki, Finland, that has 1532 nm peak absorption of 80 dB/m and numerical aperture of 0.13.

## 4. Experimental analysis

In this subsection we show first how gain alters the transmission characteristics of an LPG in line with predictions made in Section 2.2. Following that, we compare experimental results and those obtained using the rigorous theoretical simulations discussed in Section 2.3.

### 4.1. Tuning of an LPG via optical gain control

This feature was demonstrated in [18] in which a 13.5 cm long LPG of 480 μm period was inscribed into a 15-cm piece of EDF (Er80-8/125 from Liekki, Finland). Fig. 5 shows obtained results for an LPG with kL=0.52π. The theoretical predictions with the gain factor being 'fitted' to get good agreement with the experiment are also shown in Fig. 5. As we see, by controlling the gain we can obtain full coupling (at the pump power of 32 mW), although the grating has strength of kL=0.52π, exactly as predicted in the theoretical analysis shown above. It is worth mentioning that as the pump current is increased from 0 mW to 32 mW, the off-resonance transmission is increased while the resonance transmission decreases. Indeed, this effect cannot be observed by simply cascading a passive LPG with an EDF-based amplifier.

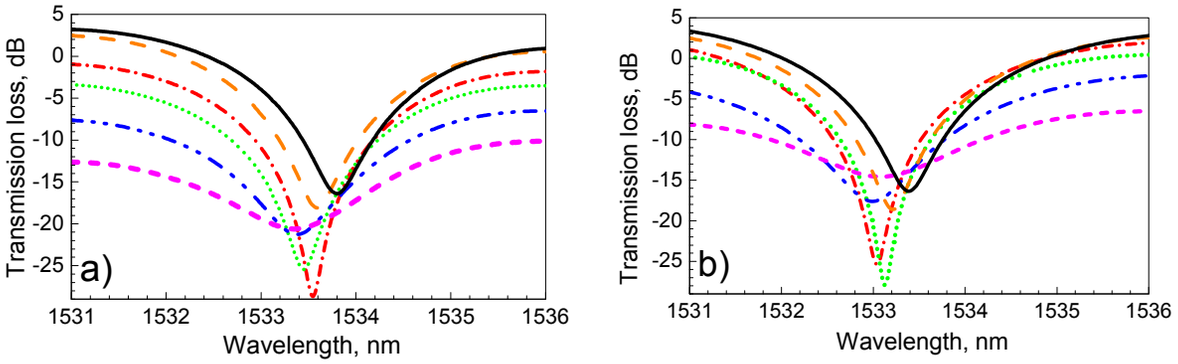


**Figure 5.** Measured (a) and calculated (b) transmission of LPG at kL=0.52π for input signal of 0.5 mW and different pump power levels (0 mW magenta, 8 mW blue, 17 mW green, 32 mW red, 145 mW orange, 220 mW black).

In practice, LPG-induced dip depth was varied from 7 dB (under-critical coupling) to the maximum of -28 dB (critical coupling) back to -18 dB (over-critical coupling) by varying the pump power between 0 and 220 mW.

### 4.2. LPG performance due to ASE and an EDF: comparison with rigorous analysis

Here we show experimental results considering an EDF theoretically modeled in the Section 2.3. Our LPG structure is shown in Fig. 6. The chosen LPG period of 480 μm corresponds to coupling into the 7$^{th}$ cladding mode.

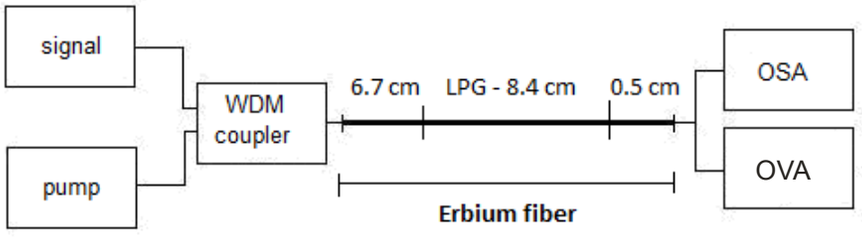


**Figure 6.** Experimental setup. OSA is optical spectrum analyzer; OVA is optical vector analyzer.

The theoretical and experimental results are shown in Fig. 7. For the critical coupling, there is about -33 dB of signal measured at the resonance in the core mode at the output, which is in a reasonable agreement with the theory that predicts -36 dB, Fig. 7b. These values are, however, significantly higher that those measured in a passive LPG, where <-60 dB was observed [14].

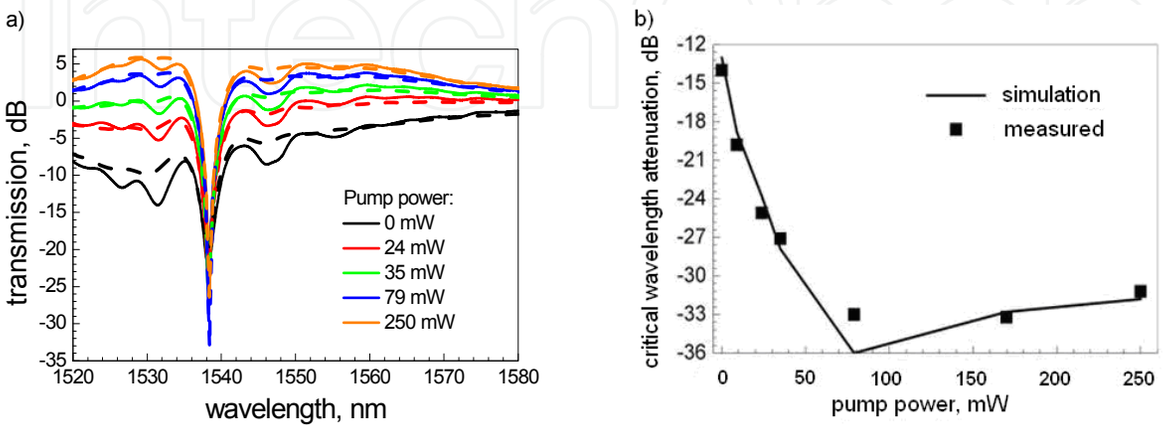


**Figure 7.** Left: experimental (solid) and theoretically computed (dashed) transmissions for various pump powers. Right: dependence of the maximum attainable resonant dip on the pump power (measured: dots; predicted: line)

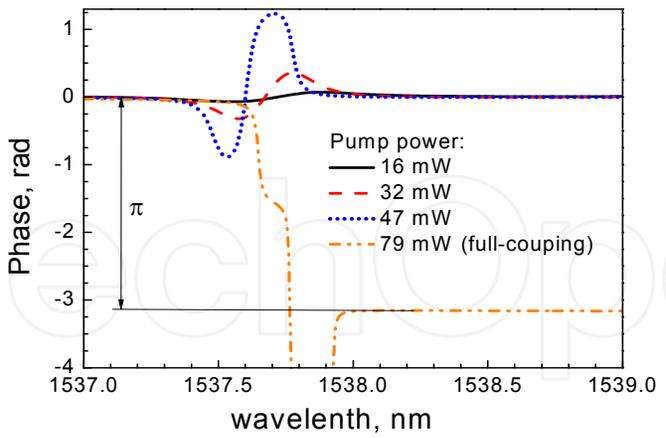


**Figure 8.** Phase characteristics of the fabricated LPG measured with optical vector analyzer (OVA, Fig. 6) for various pump powers.

To confirm that the lower level of the transmission loss for an active-fiber based LPG as compared to a passive-fiber-based LPG is due to ASE rather than any other effect (e.g., non-uniformity of the LPG due to pump power depletion across the LPG length), we measured

the phase of the transmitted light around the resonant wavelength, Fig. 8. Theory predicts that full coupling should be manifested itself as a $\pi$ phase jump across the resonance. As seen in Fig. 8, a $\pi$ phase-shift was observed confirming the grating is operated at the critical coupling condition in which all the light from the fiber core mode is out-coupled. This confirms that the residual light in the core mode at the resonance wavelength (which is close to -33 dB, Fig. 7) has to be due to ASE rather than due to limited coupling ability of the LPG.

## 5. Applications

Several applications of LPGs in active fibers have been proposed. LPG directly-written into an EDF was suggested to perform flattening of the uneven EDF gain [1]. Tuning of the transmission characteristics of an LPG via optical pumping, which has been discussed in detail above, was reported in several reports (e.g.,[18-20]). This may be of interest in many applications, including all-optical signal processing, where besides active control of the grating parameters, it is advantageous to simultaneously filter and compensate for the loss that is due to the filtering process. We discuss in detail an example of an all-optical signal processing (all-optical differentiator) [20] later. Other applications are in fiber lasers, taking advantage of the fact that cladding modes have special dispersion properties that are suitable for controlling dispersion in mode-locked fiber lasers and also have large modal areas that can be exploited in high-power fiber lasers and amplifiers [21]. Another application is in using higher order modes for high-power optical amplification. In [16], the pump and the signal were simultaneously converted into a higher-order mode (a cladding mode of an inner-cladding of a dual-cladding fiber) – the LPGs for mode conversion were written in the EDF, which was doped with active ions simultaneously in the core and in the cladding.

### 5.1. All optical differentiation

Differentiation of the $N^{th}$ order is mathematically described as $\partial^n u(t)/\partial t^n$, where $u(t)$ is the complex envelope of an arbitrary input signal spectrally centered at $\omega_0$. The corresponding Fourier spectrum can be expressed as $(-j(\omega-\omega_0))^N U(\omega)$, where $U(\omega)$ is the spectrum of the input signal $u(t)$, $\omega$ is the optical frequency ($\omega-\omega_0$ is then the baseband). Therefore $N$-th order differentiation in optical domain can be obtained using a linear optical filter with a spectral transfer function proportional to $(-j(\omega-\omega_0))^N$. Unfortunately, such filter has zero transmission at the signal carrier $\omega_0$, resulting in poor energetic efficiency (EE) defined as the ratio of the signal power after and before the differentiator. In practice, it was found that EE is <5% for an LPG-based differentiator [22]. This was confirmed by later experiments, in which some applications of this device for all-optical signal processing [23] were suggested. High order differentiation can be also realized using LPGs [24] by introducing $\pi$ phase-shifts along the LPG. However, EE is getting worse as the order of the differentiation increases [24]. Obviously, LPG written in an active fiber could be very helpful in overcoming this issue.

Let us discuss advantages of LPGs directly written into active fibers on an example of optical differentiators. The use of a passive grating in conjunction with an amplifier at its output could lead to high levels of generated ASE inside the amplifier due to low EE of the differentiation process. In the case of pre-amplification of the signal prior to differentiation, emerging nonlinearities may severely impair the output signal. E.g., for pulses with FWHM < 1 ps, nonlinearities could be observed even for modest average powers. Ideal setup is thus a configuration where we perform amplification and filtration simultaneously which is the case of LPGs in active optical fibers. Indeed, the additional flexibility by tuning the LPG via controlling pump power should be also considered.

In general, the LPG structure in an active fiber is formed by a preamplifier (active fiber before the LPG), the active grating (LPG) and a post amplifier (active fiber after the LPG). Thus it is necessary to find optimal position of the grating within the active fiber to avoid the undesirable phenomena – low signal buried in the noise on one side and emerging nonlinearities on the other. In the process of designing it is necessary to take into account: total length of EDF, position of the grating within the EDF and input signal power. The total length of EDF influences the resulting gain of the output signal. Next two parameters (position of LPG and input signal power) are to be considered in combination for minimizing the ASE and avoid nonlinearities.

For theoretical analysis [4] we have chosen LPG sample with the following parameters [20]: coupling into the seventh cladding mode (the required grating period $\Lambda$=470 μm to obtain maximum coupling at 1540 nm); LPG length of 8 cm, which corresponds to the available bandwidth for differentiation to 500 GHz; input signal is Gaussian with FWHM=1.6 ps; length of EDF S=55 cm and pumping at 976 nm with power of 200 mW. In the simulation two levels of signal power were used – low (100 μW) and high (1 mW), because studied characteristics significantly differ for different levels of signal.

Energetic efficiency as a function of LPG position within EDF for two levels of signal power is shown in Fig. 9a.

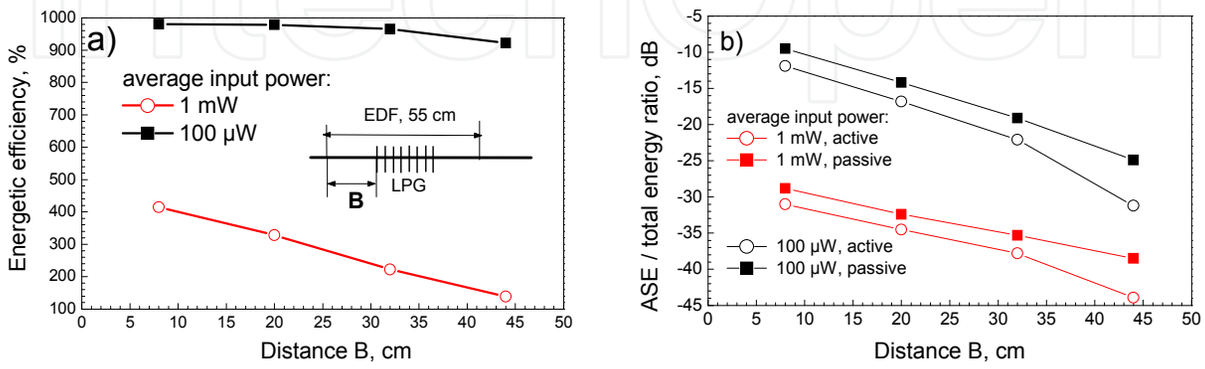


**Figure 9.** (a) Energetic efficiency for two levels of input signal power, (b) noise characteristics for EDF with embedded passive or active LPG.

For relatively low input powers the EE is practically independent from position of the grating along the fiber. For higher signal powers the dependence on the position of LPG is clearly visible (when the grating is at the beginning or end of the fiber, EE reaches 400%and 120%, respectively). The higher EE for the grating at the beginning of EDF is compensated by worse noise characteristics as shown on Fig. 9b.

For low input power (100 μW) the ratio of ASE to the total energy (ASE+signal) at the resonance drops from -12 dB (for LPG at the beginning of EDF) to -31 dB (for LPG at the end of EDF). For higher input signal power the ASE suppression is better ranging from -31 dB (LPG at the beginning of the EDF) to -44 dB (LPG at the end of the EDF). Thus, an LPG placed at the end of EDF gets the lowest ASE, while unfortunately also having the lowest EE. This trade-off between ASE suppression and EE has to be considered depending on the requirements of a particular application.

It is interesting to compare the studied design (LPG within EDF) with a design in which a passive LPG (written in a passive fiber) would be combined directly with an pre- and post-amplifier. We consider preamplifier of length B, passive LPG with the same length of 8 cm and post-amplifier with length S-B in order to get the same amplification at the end of the structure. The input signal power is the same for both cases (passive and active LPG). Comparison, Fig. 9b, shows that the passive model has – in contrast to the active model – 2 to 4 dB worse noise characteristics.

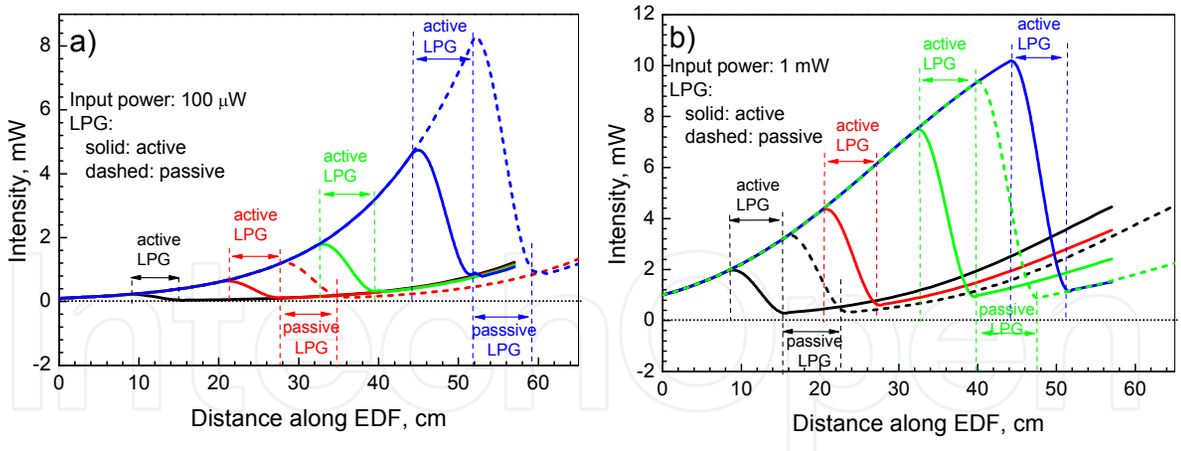


**Figure 10.** Power evolution for four different relative positions of the LPG along the EDF (black, red green and blue lines) for (a) 100 μW and (b) 1 mW input power. The performance considering a passive-fiber based LPG is shown as dashed lines.

For keeping nonlinearities low, it is necessary to minimize signal peak power along the EDF, which practically means keeping approximately constant level of the signal along the EDF. Fig. 10a shows the signal intensity for different position of the LPG within the EDF and the input signal power of 100 μW. At the same time it is shown that for the passive grating and

the same length of EDF there are positions within the fiber with increased level of power and hence possible nonlinearities. Similarly we can observe such increased levels also for input signal power of 1 mW (Fig. 10b), although they are not as significant as in case of the weak input power. From Fig. 10 one can see that for preserving the same level of intensity along the fiber it is advantageous to place the LPG close to the middle or in the first quarter of the EDF for relatively low (100 μW) and high (1 mW) input signal power levels, respectively.

Experimental realization of a differentiator in an active LPG was reported in (Krcmarik et al., 2009). The differentiator was optimized for bandwidth of 1 THz (LPG length of 3.9 cm) and relative high input power levels (LPG within the first quarter of the EDF). The entire EDF length was 35 cm to obtain EE in excess of 100% (so-called 'loss-less differentiation'). Experimental results obtained using 0.9-ps FWHM pulses of 2 mW average power are shown in Fig. 11. For comparison, performance of an ideal differentiator is also shown there.

EE of 151% was measured. However, when the input signal was launched from the opposite side of the fiber, the EE dropped to 72%, exactly in line with the theoretical predictions discussed earlier. The processed pulse demonstrates very close fit to the theoretically predicted waveform. A sharp $\pi$-phase jump in the LPG transmission necessary for accurate differentiation was also observed.

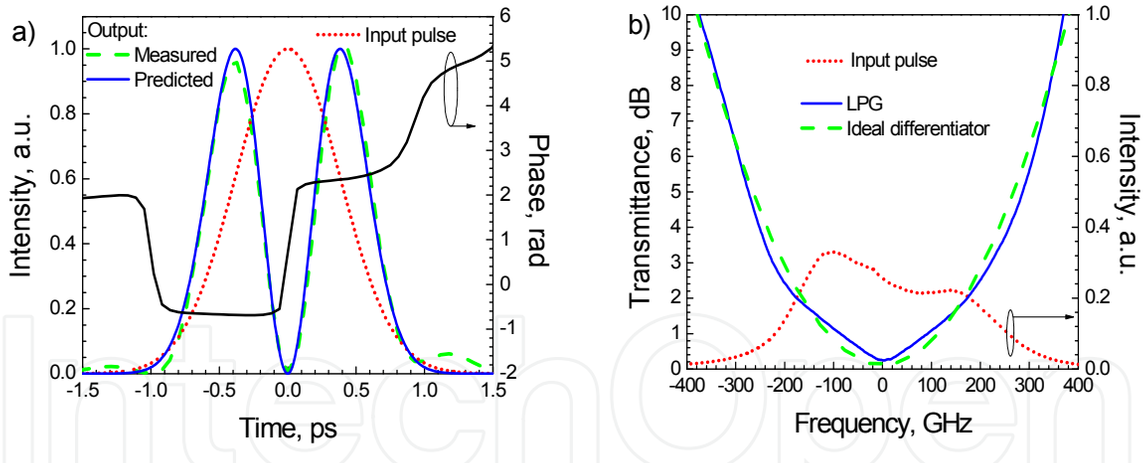


**Figure 11.** (a) Experimental and theoretical performance in time domain [20] measured phase characteristics [25] are also shown, (b) transmittance of the LPG in the vicinity of the resonance wavelength and input pulse spectrum showing that it fits entirely into the spectral region where the LPG transmittance follows the theoretically required shape.

For evaluation of the error between the ideal and the measured waveform we used square quadratic deviation formula [26]. For forward direction the error was 2.4% (Fig. 11) and for the reversed direction the error was 2.9%.

Realizing 'loss-less' higher-order differentiators, as well as characterizing experimentally the sensitivity to non-linearities are subject to further research.

## 6. Conclusions

Simultaneous diffraction and gain brings many interesting new features that are still waiting to be exploited. This chapter gives a brief overview over the state-of-the art and summarizes the key properties of long period gratings made in active optical fibers.

## Author details

David Krčmařík
*Institute of Photonics and Electronics AV CR, v.v.i, Praha, Czech Republic*

Mykola Kulishov
*HTA Photomask, 1605 Remuda Lane San Jose, CA, U.S.A.*

Radan Slavík
*Institute of Photonics and Electronics AV CR, v.v.i, Praha, Czech Republic*
*Optoelectronics Research Centre, University of Southampton, Southampton, Great Britain*

## 7. References

[1] Singh R, Sunanda, Sharma EK. Gain flattening by long period gratings in Erbium doped fibers. Optics Communications 2004; 240 (1-3), 123-132.

[2] Daxhelet X, Kulishov M. Theory and practice of long-period gratings: when a loss becomes a gain. Optics Letters 2003; 28 (9) 686-688.

[3] Kulishov M, Grubsky V, Schwartz J, Daxhelet X, Plant DV. Tunable waveguide transmission gratings based on active gain control. IEEE Journal of Quantum Electronics 2004; 40 (12), 1715-1724.

[4] Krčmařík D, Slavík R, Karásek M, Kuslishov M. Theoretical and experimental analysis of long-period fiber gratings made directly into Er-doped active fibers. Journal of Lightwave Technology 2009; 27 (13), 2335-2342.

[5] Marcuse D. (1991). *Theory of dielectric waveguides (2nd edition) – chapter 2,* Academic Press, ISBN 0124709516, New York

[6] Kong M, Shi B. Field solution and characteristics of cladding modes of optical fibers. Fiber and Integrated Optics 2006; 25 (4), 305-321.

[7] Erdogan T. Cladding-mode resonances in short- and long-period fiber grating filters. JOSA A 1997; 14 (8), 1760-1773.

[8] Thyagarajan K, Anad JK. A novel design of an intrinsically gain-flattened erbium doped fiber. Optics Communications 2000; 183 (5-6), 407-413.

[9] Jiang C, Hu W, Zeng Q. Numerical analysis of concentration quenching model of $Er^{3+}$-doped phosphate fiber amplifier. IEEE Journal of Quantum Electronics 2003; 39 (10), 1266-1271.

[10] Blixt P, Nilsson J, Carlnas T, Jaskorzynska B. Concentration-dependent upconversion in $Er^{3+}$-doped fiber amplifiers: experiments and modeling. IEEE Transaction Photonics Technology Letters 1991; 3 (11) 996-998.

[11] Myslinky P, Nguyen D, Chrostowski J. Effects of concentration on the performance of Erbium-doped fiber amplifiers. Journal of Lightwave Technology 1997; 15 (1), 112-120.

[12] Desurvire E. Study of the complex atomic susceptibility of Erbium-doped fiber amplifiers. Journal of Lightwave Technology 1990; 8(10), 1517-1527.

[13] Karásek M., Čtyroký J. Design considerations for $Er^{3+}$-doped planar optical amplifiers in silica on silicon. Journal of Optical Communications 1995; 16 (3), 115-118.

[14] Slavík R. Extremely deep long-period fiber grating made with $CO_2$ laser. IEEE Photonis Technology Letters 2006; 18 (16), 1705-1707.

[15] Rego G, Falate R, Santos JL, Salgado HM, Fabris JL, Semjonov SL, Dianov EM. Arc-induced long-period gratings in aluminosilicate glass fibers. Optics Letters 2005; 30 (16), 2065-2067.

[16] Nicholson JW, Fini JM, DeSantolo AM, Monberg E, DiMarcello F, Fleming J, Headley C, DiGiovanni DJ, Ghalmi S, Ramachandran S. A higher-order-mode Erbium-doped-fiber amplifier. Optics Express 2010; 18(17), 17651-17657.

[17] Wikszak E, Thomas J, Burghoff J, Ortac B, Limpert J, Nolte S, Fuchs U, Tünnermann A. Erbium fiber laser based on intracore femtosecond-written fiber Bragg grating. Optics Letters 2006; 31 (16), 2390-2392.

[18] Slavík R, Kulishov M. Active control of long-period fiber-grating-based filters made in erbium-doped optical fibers. Optics Letters 2007; 32 (7), 757-759.

[19] Quintela A, Quintela MA, Jauregui C, Lopez-Higuera JM. Optically tunable long-period fiber grating on an $Er^{3+}$ fiber. IEEE Photonics Technology Letters 2007; 19 (10), 732-734.

[20] Krčmařík D, Slavík R, Park Y, Kulishov M, Azaña J. First-order loss-less differentiators using long period gratings made in Er-doped fibers. Optics Express 2009; 17 (2), 461-471.

[21] Sáez-Rodriguez D, Cruz JL, Díez A, Andrés MV. Fiber laser with combined feedback of core and cladding modes assisted by an intracavity long-period grating. Optics Letters 2011; 36 (10), 1839-1841.

[22] Kulishov, M., Azaña, J. (2005). Long-period fiber gratings as ultrafast optical differentiators. *Optics Lett.*, Vol. 30, No. 20, pp. 2700-2702, ISSN 0146-9592

[23] Slavík, R., Park, Y., Azaña, J. (2007). Tunable dispersion-tolerant picosecond flat-top waveform generation using an optical differentiator. *Opt. Express*, Vol. 15, No. 11, pp. 6717-6726, ISSN 1094-4087

[24] Kulishov M, Krčmařík D, Slavík R. Design of terahertz-bandwidth arbitrary-order temporal differentiators based on long-period fiber gratings. Optics Letters 2007; 32 (20), 1715-1724.

[25] Park Y, Li F, Azaña J. Characterization and optimization of optical pulse differentiation using spectral interferometry. IEEE Photonics Technology Letters 2006; 18 (17), 1798-1800.

[26] Ngo NQ, Yu SF, Tjin SC, Kam CH. A new theoretical basis of higher-derivative optical differentiators. Optics Communications 2003; 230 (1-3), 115-129.



IntechOpen